CHAPTER VIII
CATALYTIC PYROLYSIS OF WASTE TIRE OVER HY/MCM-41 CORE-SHELL COMPOSITE

8.1 Abstract

The catalytic pyrolysis of waste tire was investigated using core-shell composite of HY and MCM-41 as a catalysts in a bench-scale reactor ramped from room temperature to 500 °C (pyrolysis zone) and 350 °C (catalyst bed), aiming to enhance the formation of petrochemicals by transformation of the bulky aromatics to valuable aromatics. The core-shell composite of HY and MCM-41 were synthesized by growing of MCM-41 over HY zeolite particles. The gaseous products were analyzed using GC-FID, whereas the GCxGC-TOF/MS and SIMDIST-GC were used for analysis of waste tire-derived oil. Moreover, the sulfur content in oils was determined by S-analyzer. It was found that The MCM-41 shell thickness was not uniform, which varied in the range of 50-100 nm. Nevertheless, the core-shell composite catalyst exhibited the great catalytic behavior in the enhancement of quality of waste tire-derived oil. The oil produced from the composite catalyst contained a higher amount of gasoline and valuable aromatics, especially ethylbenzene and toluene than the pure HY and MCM-41 catalysts, indicating the existence of bimodal pore size distribution and good balance of acidity between micropore and mesopore layers of core-shell composite exhibits a higher cracking activity and better petrochemical selectivity than pure HY and MCM-41 catalyst. Furthermore, the core-shell catalysts also provided a lower sulfur content in oil than the both HY and MCM-41 catalyst. Therefore, the core-shell composite of HY and MCM-41 has a great potential in producing petrochemical-rich oil with a low sulfur content from waste-tire pyrolysis.

8.2 Introduction

Nowadays, the energy consumption continuously increases, and the fossil fuel is not a sustainable resource for production of fuels and petrochemical feedstock. Therefore, researchers attempted to seek for alternative fuels and petrochemical feedstock resources. Among all alternative resources, waste tire is highly attractive because it mainly consists of hydrocarbons, which can be directly converted to useful products by pyrolysis. The products, which are obtained from pyrolysis of waste tire, are composed of gas, liquid oil and solid char. The liquid or tire-derived oil is much more interesting than the gas and char products since it contains valuable petrochemicals such as benzene, toluene, and xylenes, and could be used as a fuel that substitutes conventional fuels. However, a significantly-high amount of polycyclic aromatic, sulfur-containing and nitrogen-containing compounds limits the use of tire-derived oil as a fuel or petrochemical feedstock.

Consequently, several researchers focused on the enhancement of petrochemical production and reduction of the poly- and polar-aromatics in tire-derived oil. For instances, Boxiong *et al.* (2007) reported that using ZSM-5 and USY zeolites selectively produced mono-aromatics, especially benzene, toluene, and xylenes. Muenpol *et al.* (2015) stated that HBETA catalyst enhanced the formation of benzene and ethylbenzene while HMOR catalyst significantly enhanced stylene production. Furthermore, HY catalyst increased the selectivity of benzene and toluene. Among those zeolites, Y-zeolite enhanced saturated hydrocarbons and mono-aromatic production, and reduced the production of di-, poly- and polar-aromatics as reported by Manchantrarat and Jitkarnka (2012), and Wehatornawee and Jitkarnka (2010). However, a relatively-high concentration of poly- and polar aromatics still remains in the tired-derived oil with using zeolites. There are two possible reasons that can explain the high formation of bulky aromatic compounds. The first reason is that the formation of aromatics increases with the increase of acidity. The second reason is that the sizes of aromatics molecules are larger than the micropore of zeolites; then, large aromatic compounds are not cracked into smaller aromatics or light hydrocarbon products. Consequently, mesoporous materials,

which have a large pore size and low acidity, are attractive to the use as a catalyst in the pyrolysis of waste tire. Mesoporous MCM-41 promoted the reduction of poly- and polar-aromatics, whereas the formation of mono-aromatics and saturated hydrocarbons increased (Dũng et al., 2009). On the other hand, another type of mesoporous material, which is SBA-1, was used as a catalyst for waste tire pyrolysis. SBA-1 did not reduce the concentration of di-, poly- and polar-aromatic in oil due to excessively weak acidity (Dũng *et al.*, 2010).

In addition, composite materials, combining advantages of both microporous zeolites and mesoporous molecular sieves, have been also developed and used to overcome the drawbacks of zeolites and mesoporous materials. Composite materials. The advantages of these materials are large pore size and high surface acidity distribution. For instance, the MCM-41/BETA composite material provided a higher cracking activity in cracking of waste palm oil, resulting in the high gasoline fraction in oil (Ooi *et al.*, 2004). Moreover, hydrocracking of heavy oil using a core-shell composite of USY and SBA-15 provided a higher liquid yield and better conversion in cracking of n-hexadecane than pure USY zeolite (Jia *et al.*, 2013). Ren *et al.* (2008) investigated the hydrodesulfurization of dibenzothiophene catalyzed by Ni-Mo sulfides supported on core-shell composites of MCM-41 and HY-zeolite. The composite catalysts were prepared by overgrowing MCM-41 over HY zeolite, and physical mixing of MCM-41 and HY zeolite. TEM images indicated that HY zeolite was covered by a thin MCM-41 layer in composite catalysts. Both composites of HY zeolite and MCM-41 gave higher hydrodesulfurization activity than HY zeolite and mesoporous MCM-41 due to the increase of surface acidity by the introduction of HY zeolite. Similarly, Li *et al.* (2009) studied hydrodesulfurization performance of Ni-Mo supported on the core-shell composite of HY and MCM-41. They found that the hydrodesulfurization via hydrogenation (HYD) pathway was significantly increased by the introduction of HY zeolite in the composite catalyst. However, the hydrocracking activities of Ni-Mo supported on the composites of HY and MCM-41 were low because the hydrodesulfurization of dibenzothiophene possibly occurred in the mesopore. Zhou *et al.* (2010) studied hydrodesulfurization of dibenzothiophene catalyzed by Pd supported on core-shell composite of MCM-41 and HY. Pd metals

supported on the composite materials exhibited the high activity and stability of hydrodesulfurization (HDS) of dibenzothiophene since the acidic support promoted HDS activities and HYD selectivity. In addition, the core-shell structure of composite materials increased the HDS performance, especially sulfur resistance.

According to the above background, the core-shell composite of HY-zeolite and mesoporous MCM-41 has high potential to be able to reduce large polycyclic aromatics and increase petrochemical products in tire-derived oil from pyrolysis of waste tire. Bulky hydrocarbons, which have larger sizes than the pore size of a zeolite, might be able to be cracked in MCM-41 shell. Smaller hydrocarbons, which are the cracking products of MCM-41 shell, later diffuse to the zeolite core to be further cracked to even much lighter hydrocarbons and valuable mono-aromatics. Therefore, the aim of this work was to investigate the effect of core-shell composite of HY and MCM-41 catalyst on the waste tire pyrolysis products in terms of oil quality improvement and enhancement of valuable petrochemical formation.

8.3 Experimental

8.3.1 Synthesis of Core-shell Composite

The core-shell structure composites of HY zeolite and MCM-41 were synthesized by the method in Li *et al.* (2009). 4.25 g of CTABr was dissolved in 40 mL of deionized water, and 1.2 g of HY was added to the solution at 25 °C with stirring for 24 h to form Slurry A. Solution B was prepared by dissolving 9.79 g of sodium silicate in 100 mL of deionized water, and the pH was adjusted to 11 by adding 6 M H_2SO_4. After stirring for 10 min, Slurry A was added drop by drop to Solution B. After that, the mixture was stirred at room temperature for 2 h and kept into an autoclave at 120 °C for 72 h. Then, the solid product was filtered, washed, dried, and calcined at 540 °C for 6 h. In the synthesis of MCM-41, the 4.25 g of CTABr was dissolved in 40 mL of deionized water, followed by the addition of the solution containing 9.79 g sodium silicate and 100 mL of deionized water. The solution of sodium silicate was priorly stirred until the solution was clear before addition to the CTABr solution. After stirring at 25 °C for 2 h, the mixture of CTABr, sodium silicate and DI water was transferred into an Teflon line autoclave at

temperature 120 °C for 3 days. Then, the solid product was filtered, washed, dried, and calcined at 540 °C for 6 h. The catalyst power were pelletized, crushed and sieved to 40-60 mesh of particle size.

8.3.2 Catalyst Characterization

The catalyst samples were characterized by different physicochemical characterization methods. X-Ray diffraction (CuKα radiation), carried out in a Rigaku TTRAXlll Diffractometer and Rikagu SmartLab X-Ray Diffractometer and, were used to collecting of the small-angled X-ray scattering (SAXS) pattern and wide-angle XRD pattern, respectively. Wide-angle XRD patterns were recorded in the 5-65 ° (2θ) range using a scan speed of 10° (2θ)/min and small-angle XRD patterns were recorded in the 2.0-6.0 °(2θ) range using a scan speed of 2° (2θ)/min. The surface area and pore volume of catalyst were measured using N_2 adsorption-desorption isotherms with Quantachrome AS1-MP instrument. Transmission electron microscopy (TEM) was performed on JEOL JEM-2010 and JEOL JEM-2011 instruments with an acceleration voltage of 200 KV. The amount of coke deposition on the spent catalysts was determined using thermogravimetric/differential thermal analysis (TG/DTA), carrier out under flowing of nitrogen (10 ml/min) and oxygen (20 ml/min) on a Perkin Elmer/Pyris Diamond (Thermogravimetric/Differental Thermal Analysis, TG/DTA). A sample was heated up from room temperature to 900 °C with the ramping rate of 10 °C/min. CHNS analyzer was used to determine the sulfur and nitrogen content on spent catalysts using LECO®Elemetal Analyzer.

8.3.3 Waste Tire Pyrolysis

The schematic pyrolysis system was displayed in Figure 8.1. Firstly, 30 g of shredded tire (20-40 mesh) was pyrolyzed in the lower zone of the reactor at 500 °C under atmospheric pressure. The pyrolysis products were carried by 30 ml/min of nitrogen flow to the catalytic bed filled with 7.5 g of catalyst and heated to 350 °C. After the temperature of lower and upper zone reached to the desired temperature, the temperature of two zones was kept for 2 h. The resulting products were separated into gas and liquid fractions by ice-salt condensing system. The gas product was collected in Tedlar PVF bag.

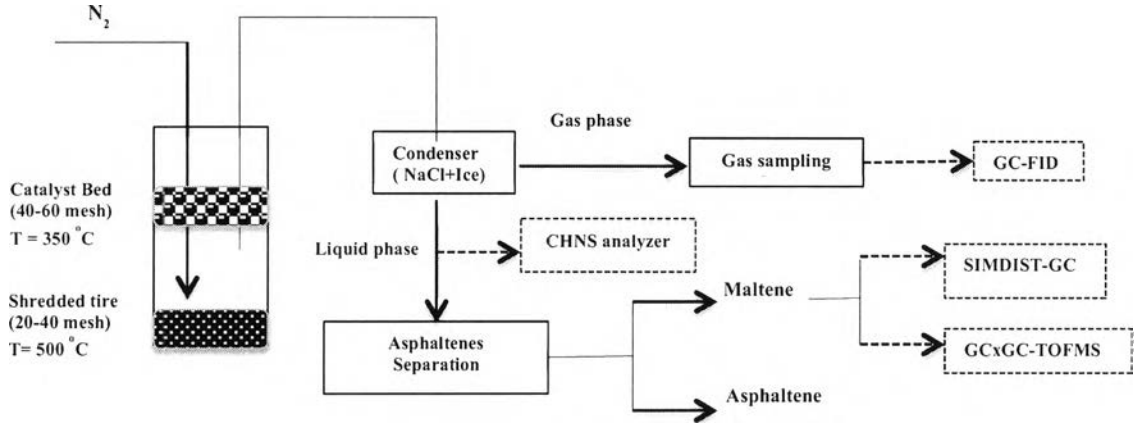

Figure 8.1 Schematic of waste tire pyrolysis system for collection and analysis of products.

8.3.4 Product Analysis

Liquid and solid products were weighed to determine the product yield. The gas yield was determined by mass balance. The gaseous product was analyzed by GC, Agilent Technologies 6890 equipped with HP-PLOT Q column (300 mm x 0.32 mmID and 20 μm film thickness) and FID detector. The liquid product was dissolved in n-pentane (mass ratio of n-pentane/oil =40:1) to precipitate asphaltene. Asphaltene was filtered by using a polyamide membrane (0.45 μm). The maltene solution was then analyzed by Comprehensive Two-Dimension Gas Chromatography (Agilent Technologies 7890) with Time-of-Flight Mass Spectrometer (LECO, Pegasus® 4D TOF/MS equipped with the 1st GC column was a non-polar Rtx®-5Sil MS (30 m x 0.25mmID x 0.25μm) and the 2nd GC column was an Rxi®-17MS(1.790m x 0.1mmID x 0.1μm). The primary column was held up at 50 °C for 2 min, and then heated up to 310 °C with a ramping rate of 5 °C/min. After final temperature was reached, it was held at 310 °C until the analysis was finished. For the secondary column, the column temperature was held at 60 °C for 2 min, and then ramped up to 320 °C with the ramping rate of 5 °C/min. After reached, the final temperature of column was held at 320 °C until the analysis was finished The simulated true boiling point curves were determined by using a Varian GC-3800 simulated distillation gas chromatography equipped with FID detector and a 15m x

0.25 mm x 0.25 μm WCOT fused silica capillary column. The petroleum fractions were cut based on their boiling point ranges according to the ASTM D2887; gasoline (<149 °C), kerosene (149-232 °C), gas oil (232-343 °C), light vacuum gas oil (343-371 °C) and heavy vacuum gas oil (>371 °C). Moreover, sulfur and nitrogen content in tire-derived oil and char were determined using LECO®Elemetal Analyzer (TruSpec®CHNS). Furthermore, sulfur content in gas product was determined from mass balance.

8.4 Results and Discussion

8.4.1 Characterization of Core-shell Composite of HY and MCM-41

The XRD patterns of HY zeolite, MCM-41 and the core-shell composite catalysts are shown in the Figure 8.2. The diffraction peak of (100) plane is clearly reflected at $2\theta = 2.1°$in the XRD patterns of both MCM-41 and HY/MCM-41 catalyst, indicating that the mesostructures are well present in the both catalyst. Furthermore, the diffraction peaks at high diffraction angles in the XRD pattern of HY/MCM-41 are similar to the XRD pattern of HY zeolite, indicating that HY zeolite is also present in the composite catalyst.

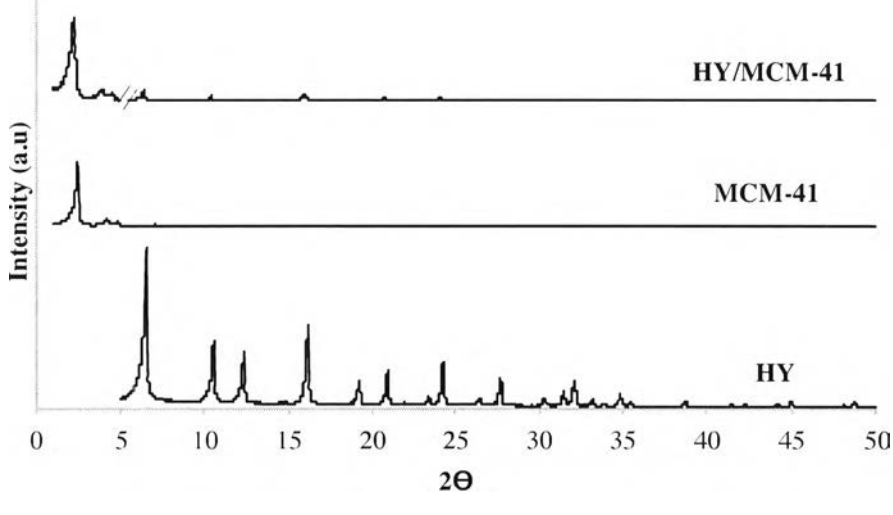

Figure 8.2 XRD patterns of HY, MCM-41 and the composite of HY and MCM-41.

The N_2 adsorption-desorption isotherms of MCM-41, HY, and HY/MCM-41catalyst are shown in Figure 8.3. HY zeolite exhibits the type I adsorption isotherm, which presents the characteristic of micropore. On the other hand, MCM-41 and HY/MCM-41 display the IV adsorption isotherms. These isotherms exhibit three steps of N_2 adsorption. The slightly rising step at $P/P_o < 0.25$ indicates the presence of micropore in both composite and MCM-41 catalysts. The steep rising step with the relative pressure P/P_o range of 0.25-0.4 results from the capillary condensation in mesopore, indicating that the framework-confined mesopores are present in the catalysts (Bordoloi *et al.*, 2006). Moreover, the slope of this step indicates the uniformity of pore size distribution. Therefore, it is reasonable to conclude that the MCM-41 catalyst has a higher uniformity of pore size distribution than the composite catalyst, which well agrees with the pore size distribution in Figure 8.4. The third step with the relative pressure P/P_o range of 0.9-1.0 indicates that the existence of macropore in the both composite and MCM-41 catalysts. However, the hysteresis loop of the composite is significantly different from that of the MCM-41 catalyst since its hysteresis is contributed by MCM-41 at P/P_o = 0.25-0.4 and 0.95-1.0 and by HY at P/P_o = 0.85-1.0. Therefore, it is reasonable to conclude that the composite material contains micropores, mesopores, and some macropores.

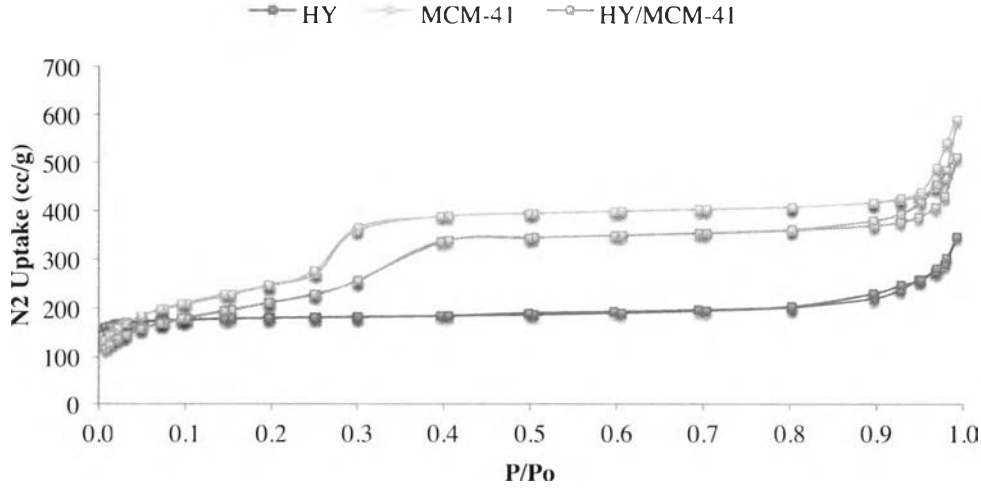

Figure 8.3 N_2 adsorption-desorption isotherms of HY, MCM-41 and HY/MCM-41 composite.

The BJH pore size distributions of MCM-41, HY, and the composite of HY and MCM-41 present the distribution in the range of 0-10 Å, indicating the existence of micropore in all three catalysts. The mesopore size distribution of MCM-41 is narrower than the HY/MCM-41 catalyst, which well agrees with the steep rise at P/P_0 range of 0.25-0.4. The textural properties, such as BET surface area, pore volume and average pore size are summarized in Table 8.1. The BET surface area of the HY/MCM-41 composite is higher than the HY zeolite but lower than MCM-41, indicating that the higher surface area of composite material is contributed from the mesopore of MCM-41.

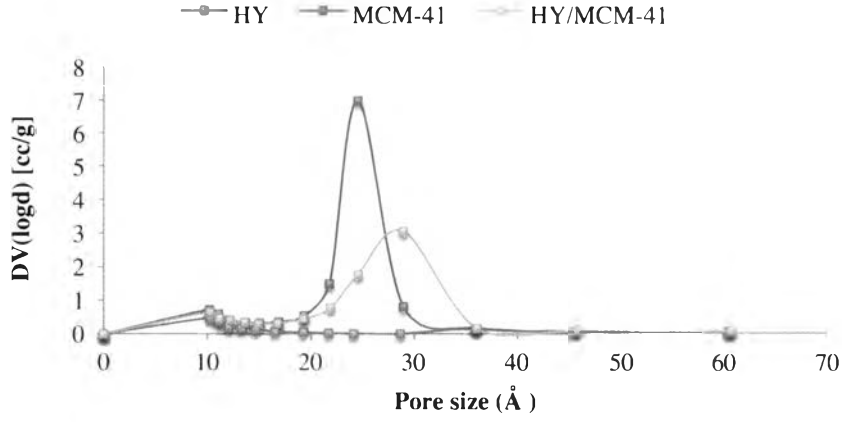

Figure 8.4 Pore size distribution of HY, MCM-41 and HY/MCM-41 composite.

Table 8.1 Textural properties of HBETA, MCM-41 and HBETA/MCM-41 composite

Catalyst	BET surface area (m2/g)	Pore volume (cm3/g)	BJH average pore size (nm)
HY	546	0.34	10.3
MCM-41	1,064	1.00	24.6
HBETA/MCM-41	790	0.85	29.0

Figure 8.5(A) and 8.5(B) display the TEM image of the composite of HY and MCM-41. It is found that the HY zeolite particles are enwrapped by the thin layer of MCM-41, which MCM-41 has a less density than the zeolite particle. However, the MCM-41 shell thickness is not uniform, which varies in the range of 50-100 nm. The average shell thickness is about 43 nm. Moreover, the energy dispersive X-ray

spectroscopy (EDS) is used to determine the chemical composition of the microporous and mesoporous phases.

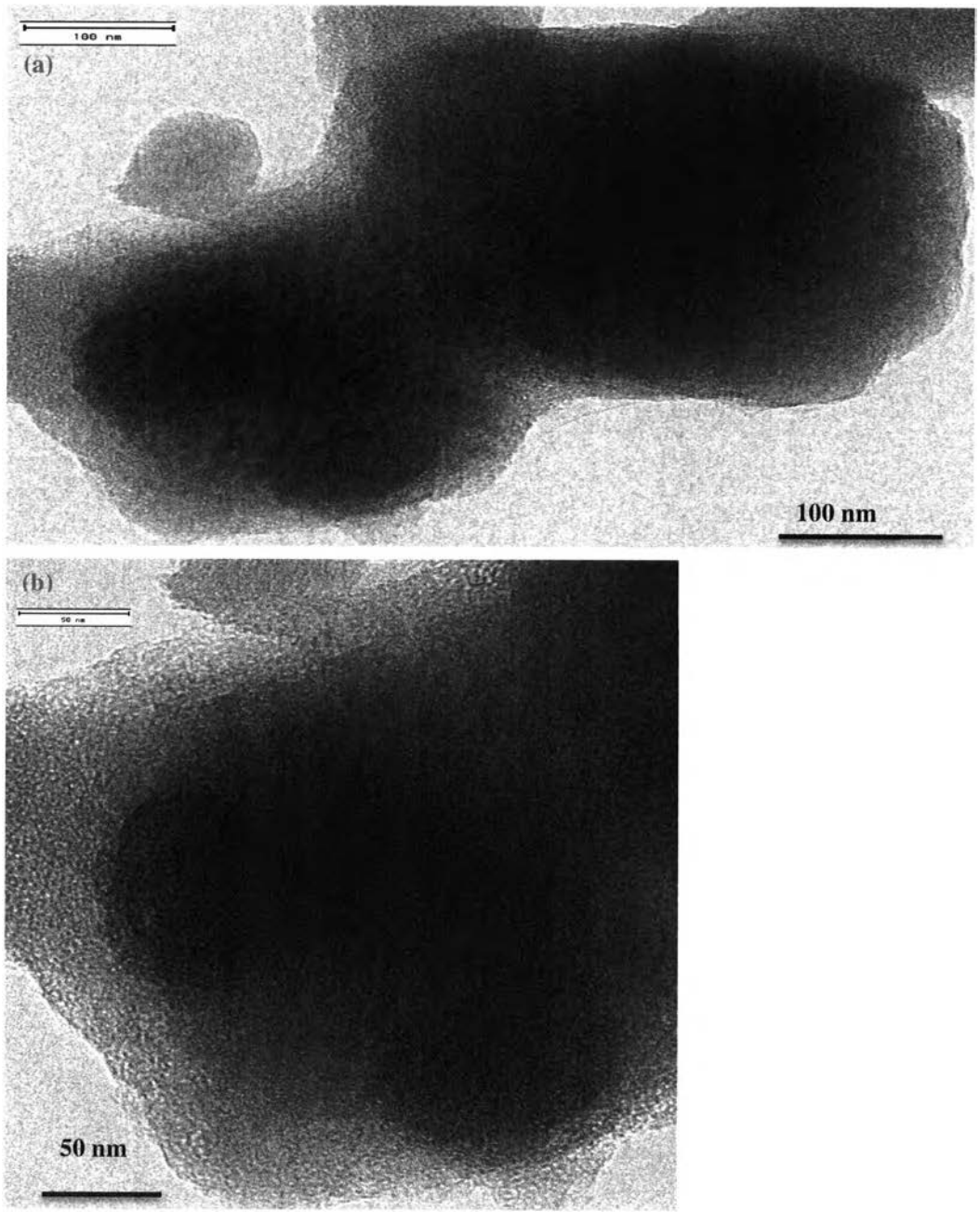

Figure 8.5 TEM image of the core-shell composite of HY and MCM-41.

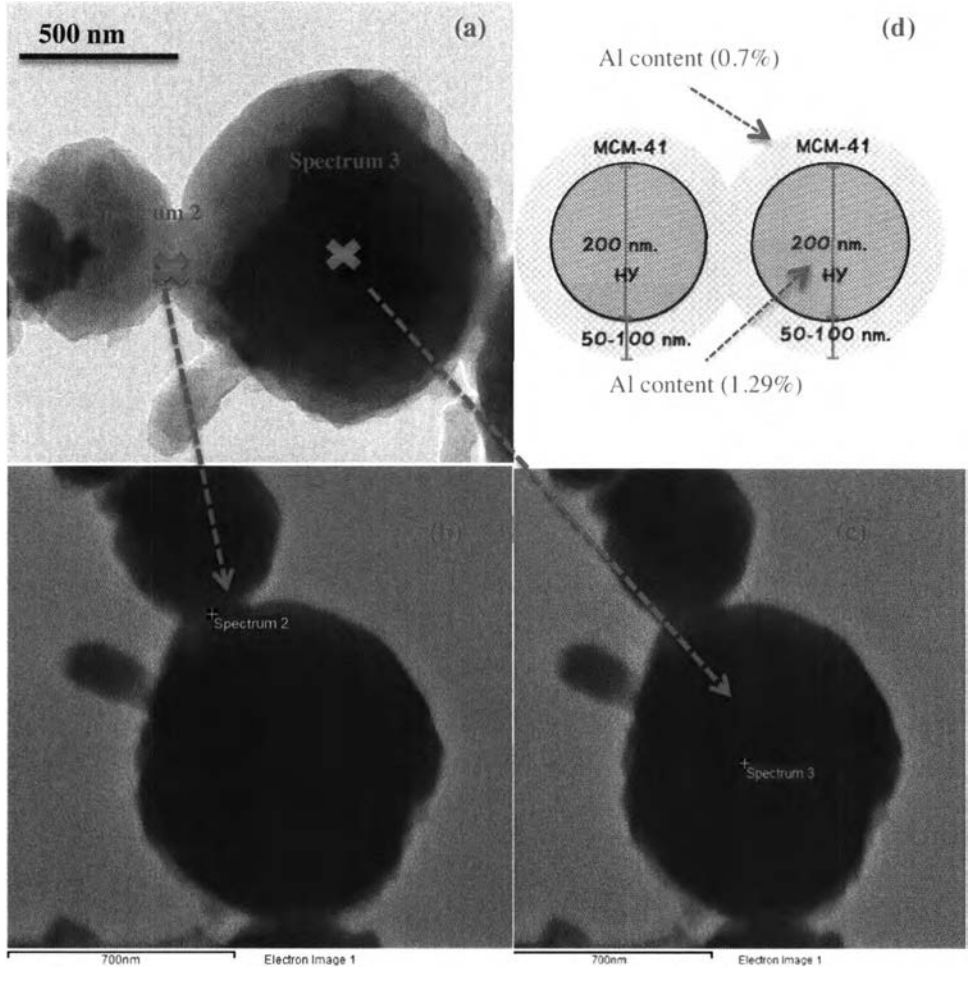

Figure 8.6 TEM image (a) and STEM images of the core-shell composite of HY and MCM-41(b,c) and drawing of core-shell composite of HY and MCM-41 (d).

Figure 8.6 displays the STEM image. After EDS was applied at the position believed as to be MCM-41 shell (see Figure 8.6(b)), the result shows that O, Na, Al, Si, Cr, Os, C and Cu elements were detected, of which Os, Cu, Cr and C elements is from the Cu grid used in the experiment. Moreover, the mass ratio of Si/Al is about 72.2 (see Figure 8.7(a)). Furthermore, the Al content at the position believed to be a HY core (see Figure 8.6(c)) is higher than the first position of MCM-41 shell, and the mass ratio of Si/Al ratio of this position is about 37.8 (see Figure 8.7(b)), which is roughly twice than the Si/Al ratio of MCM-41 shell. It is well known that the MCM-41 is silica material, so the Al content of MCM-41 shell should be nearly equal to

zero. However, some Al content is found in the MCM-41 shell since somes Al content in MCM-41 shell come from Al_2O_3 in sodium metasilicate, which is used as a silica source (Li *et al.*, 2009). In addition, some overlapping of MCM-41 and HY layers might take place at the position that EDS was taken, leading to the higher content of Al in MCM-41 shell. Therefore, it is reasonable to conclude that the composite catalyst containing MCM-41 and HY core has been successfully synthesized.

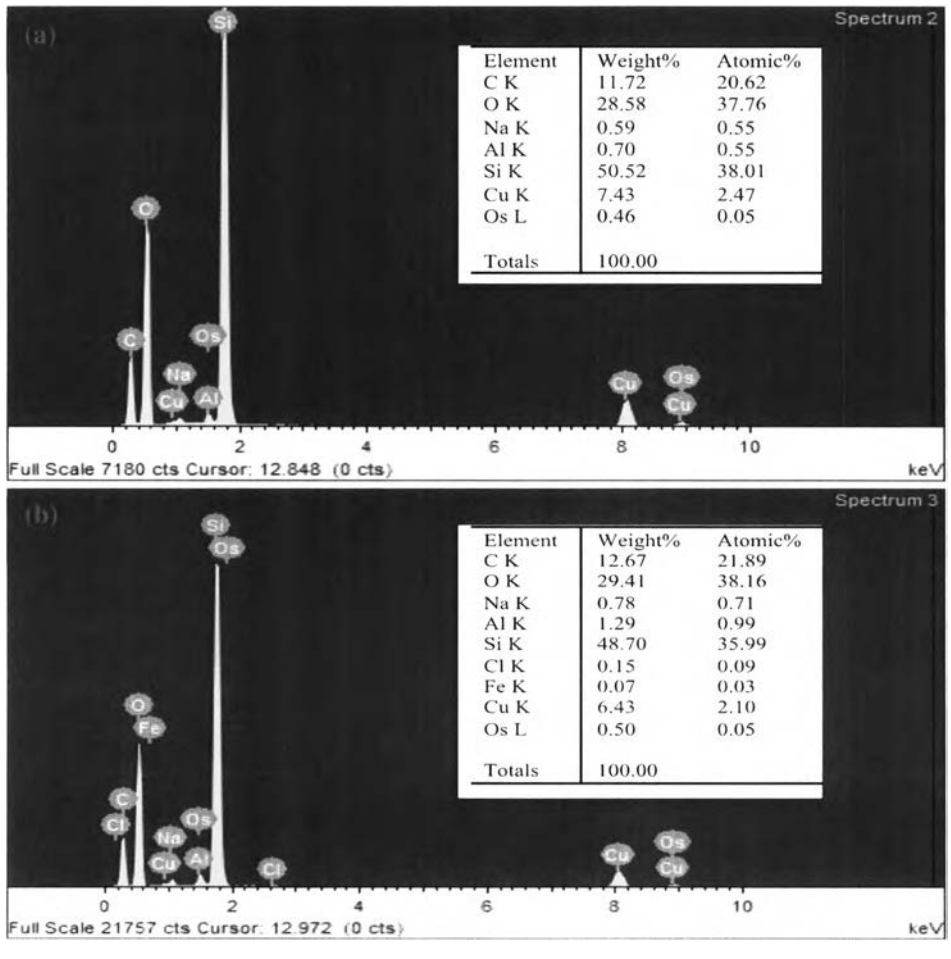

Figure 8.7 EDS spectra of MCM-41 shell (a) and HY core (b).

8.4.2 Pyrolysis Yields

The pyrolysis product distributions from using parent HY zeolite, MCM-41, and HY/MCM-41 catalysts are displayed in Figure 8.8(a). The core-shell composite of HY and MCM-41 maintains the liquid yield, but suppresses the gas yield, due to the coke formation as compared to thermal pyrolysis. HY catalyst clearly provides a higher yield of gas and a lower liquid yield than those obtained from MCM-41 catalyst since the HY zeolite possesses strong acid sites and high acid density, so it provides a higher cracking activity than MCM-41 that possesses only weak acid sites. However, the difference of the product distributions from all catalysts are found on the gas yield resulted from the coke formation. These observations indicate that the growth of MCM-41 shell around HY core provides a higher cracking activity than the parent MCM-41 catalyst and enhances resistance of coke formation. It can be explained that the mesoporous MCM-41 shell might provide free channel for cracking products to diffuse out of the HY core, resulting in reduction of excessive cracking, which leads to a lower coke formation on the catalyst and a higher yield of liquid.

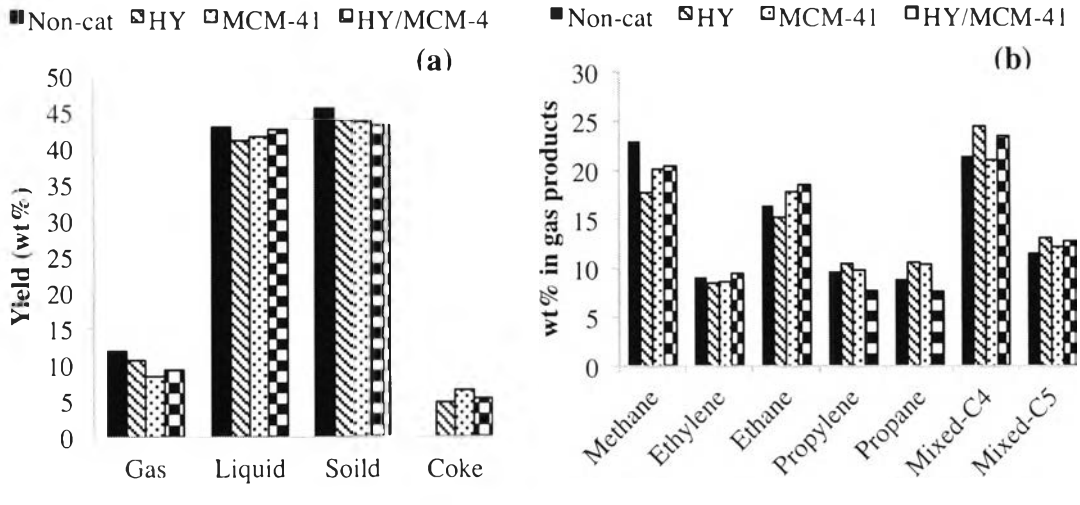

Figure 8.8 Pyrolysis yields (a) and compositions of gaseous products from using HY, MCM-41 and the HY/MCM-41 core-shell composite (b).

The amount of mixed-C4 and mixed-C5 gases can be a one of indicator that indicates the cracking ability of catalysts since the mixed-C4 and mixed C5, which

are rubber monomers of tire molecules, can be directly formed by breaking of carbon-carbon bond of styrene-butadiene and isoprene rubbers. For the parent MCM-41, propane, ethane, propylene and mixed-C5 increases, whereas the other gaseous products decrease as compared to the non-catalytic case (see Figure 8.8(b)). The presence of core-shell composite of HY zeolite and MCM-41 provides a higher formation of mixed-C4 and mixed-C5 gases than those produced by the parent MCM-41 catalyst since the hydrocarbon molecules might be cracked by MCM-41 shell, and then further cracked by the zeolite core, leading to the higher formation of lighter hydrocarbon products. The presence of HY catalyst significantly enhances the formation of propane, propylene, mixed-C4 and mixed-C5 gases, which are higher than those obtained from MCM-41 catalyst. Therefore, the single dimension connection of HY zeolite with MCM-41 shell can provide a higher cracking activity of catalysts than MCM-41 catalyst.

8.4.3 Waste Tire-derived Oil

Figure 8.9 provides the information about the composition in maltenes. MCM-41 with mesopore and weak acid sites provides higher amounts of mono-aromatics, olefins and paraffins, whereas the amounts of di-and poly-aromatics, and napthenes decrease as compared to the non-catalytic case. These results indicate that the low acidity of MCM-41 catalyst can also promote the aromatization of naphthenes, leading to the formation of mono-aromtics. It can be explained that the cracking ability of MCM-41 associates with silanol group, which generates carbenium ions when interact with hydrocarbon molecules. Moreover, the mesopore of MCM-41 clearly promotes the transformation of heavy aromatics, such as di- and poly-aromatics to lighter aromatic, olefins and paraffins. Parent HY zeolite produces higher amounts of mono-, and di-aromatics, but provides lower amounts of naphthenes and olefins than the non-catalytic case, indicating that HY with micropore pore and strong acid sites favors the formation of mono- aromatics via two pathways; cracking of poly-aromatics and aromatization of naphthenes and olefins.

The presence of the core-shell composite of HY and MCM-41 provides a higher amount of olefins and naphthenes than the pure HY and MCM-41 catalysts. Moreover, the concentration of mono-aromatics is quite similar to those obtained from MCM-41, whereas the concentrations of poly- and polar-aromatics clearly decrease as compared to those obtained from pure HY and MCM-41 catalysts. In addition, an olefin, 1,5-Heptadien-3-yne, has been found to significantly increase in the presence of the core-shell composite of HY and MCM-41, but has been not found in the oils produced by HY and MCM-41 catalysts. These results indicate that the presence of single dimension connection between MCM-41 shell and HY core provides a higher cracking activity than pure HY and MCM-41 catalysts, resulting in the higher conversion of polycyclic aromatics and mono-aromatics to more lighter products (olefins and naphthenes). It can be explained that the connection of two different pore sizes of the composite catalysts can decrease the formation of di-, poly- and polar-aromatics in maltene as compared to HY zeolite, which only possesses micopores In addition, the cracking products, which escape from the HY core, can be further cracked in MCM-41 shell, resulting in the formation of lighter hydrocarbon products such as olefins and naphthenes. Moreover, the higher reduction of concentration of mono-aromatics in the presence of core-shell composite catalyst than HY zeolite clearly indicate that the cracking products, especially mono-aromatics, that previously cracked in HY core might be further cracked in MCM-41 shell, resulting in high formation of olefins and paraffins. Therefore, it is reasonable to conclude that the presence of the core-shell composite of HY and MCM-41 provides a higher cracking activity than the pure HBETA and MCM-41, resulting in the enhancement of quality of tire-derived oil.

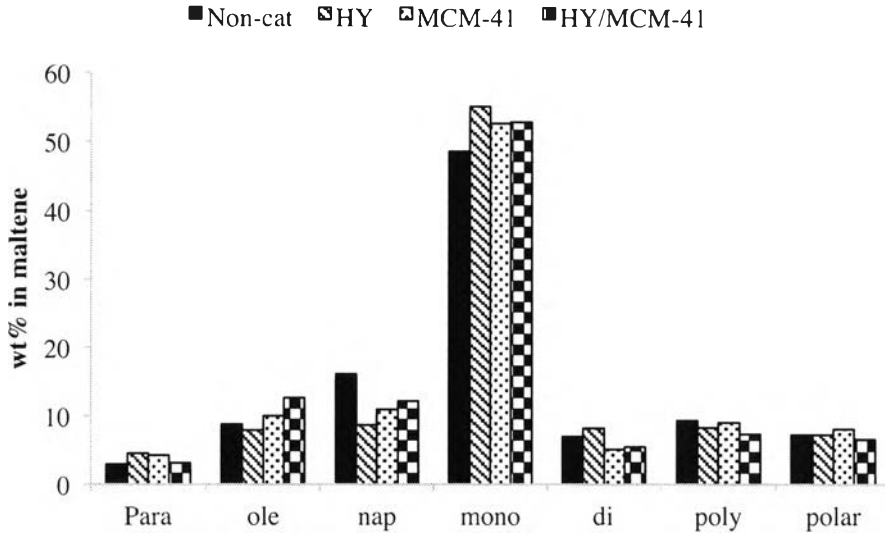

Figure 8.9 Maltene compositions (pare=paraffins, ole=olefins, nap=naphthenes, mono=mono-aromatic, di=di-aromatics, poly=poly-aromatics, and polar=polar-aromatics) from using HY, MCM-41 and the HY/MCM-41 core-shell composite.

From Figure 8.10, the pure HY zeolite provides the lighter oil with higher proportion of gasoline and kerosene than the non-catalytic case. However, with using pure MCM-41 as a catalyst, the gasoline fraction is higher than those obtained from pure HY zeolite, while the fraction of kerosene is lower than using HY as a catalyst. Therefore, it can be concluded that the larger pore size of MCM-41 allows hydrocarbons in kerosene fraction that have a quite large molecular size, which cannot be sufficiently cracked in micropore of zeolite, to diffuse inside to be cracked into the lighter gasoline range hydrocarbon products. In addition, the presence of the core-shell composite of HY and MCM-41 provides the highest amounts of gasoline whereas the amounts of gas oil, LVGO and HVGO are the lowest among all catalysts. These results indicate that some heavy hydrocarbons can be cracked at the weak acid sites of MCM-41 shell into smaller hydrocarbons, which can next effectively diffuse to the zeolite core, and then the smaller hydrocarbons are further cracked at the strong acid sites of HY core, resulting in the lightest product.

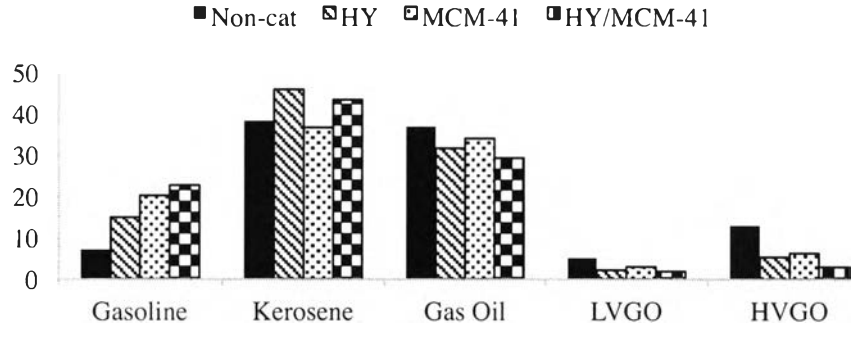

Figure 8.10 Petroleum fractions in maltene from using HY, MCM-41 and the HY/MCM-41 core-shell composite.

Regarding to petrochemical species in maltene, the pure HY zeolite itself enhances the formation of ethylbenzene, toluene, mixed-xylenes and styrene in maltene. On the other hand, pure MCM-41 also enhances the formation of ethylbenzene, toluene, mixed-xylenes, cumene and styrene in maltene. Although the concentration of mono-aromatics in maltene produced by the core-shell composite is lower than that obtained from HY zeolite, and nearly equal to that obtained from MCM-41 catalyst, the core-shell composite significantly enhances the selectivity of ethylbenene and toluene in maltene (See Figure 8.11).

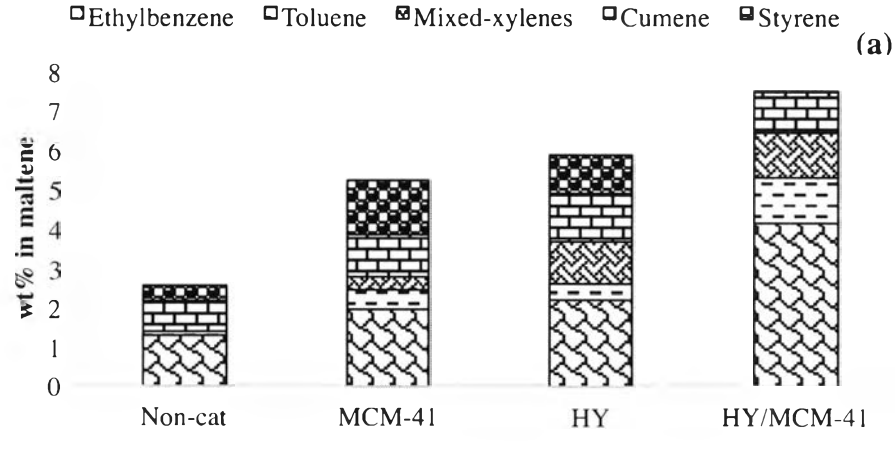

Figure 8.11 Concentration of petrochemicals in maltenes (a), and concentration of mono and poly-aromatics from using HY, MCM-41 and the HY/MCM-41 core-shell composite (b).

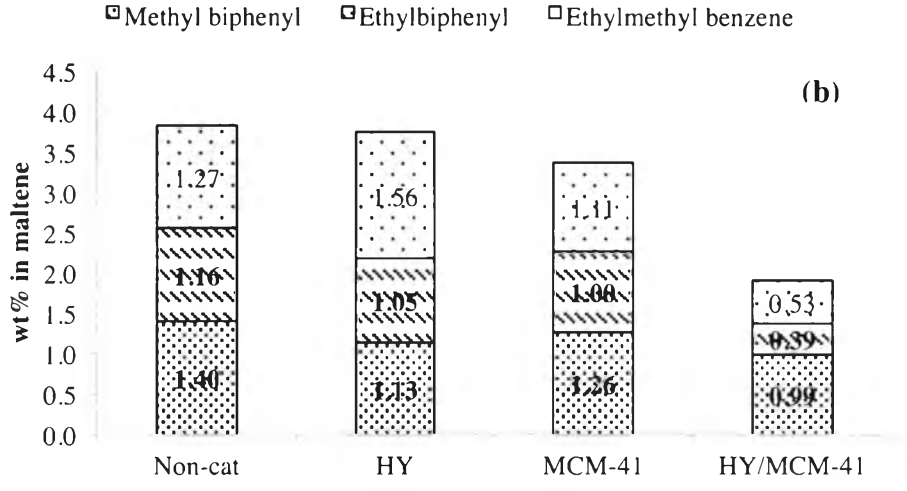

Figure 8.11 Concentration of petrochemicals in maltenes (a), and concentration of mono and poly-aromatics from using HY, MCM-41 and the HY/MCM-41 core-shell composite (b). (Con't.)

The presence of the composite catalyst promotes the transformation of mono-, poly- and polar aromatics to valuable petrochemicals since some heavy aromatics are cracked at the weak acid sites of MCM-41 to form intermediate aromatics, which then can diffuse more effectively to the zeolite core of HY and are further cracked on the strong acid sites of HY zeolite, resulting in the formation of valuable aromatics. Moreover, the MCM-41 shell might provide some free channels that allow some valuable aromatics escaping from HY zeolite to diffuse through MCM-41 channel without further transformation. Simultaneously the reductions of some poly-aromatics and mono-aromatics species such as ethylbiphenyl, methylbiphenyl, 1-ethyl-3-methyl-benzene and etc were observed. It is proposed that the high formation of ethylbenzene in the maltene can be resulted from the cracking of ethylbiphenyl as displayed in **Scheme 1**. After the carbon-carbon scission at the position between two benzene rings, ethylbenzene and benzene radical can be directly formed. If the H_2 can be produced sufficiently, radicals of benzene can be reacted with H_2 to form benzene. However, the concentration of benzene has not been found to increase, so the benzene radical might react with other active hydrocarbons, forming other hydrocarbon species. This reaction pathway likely takes

place on both MCM-41 shell and HY core since the pure MCM-41 and HY zeolite also reduce the formation of ethylbiphenyl (see Figure 8.11(b)).

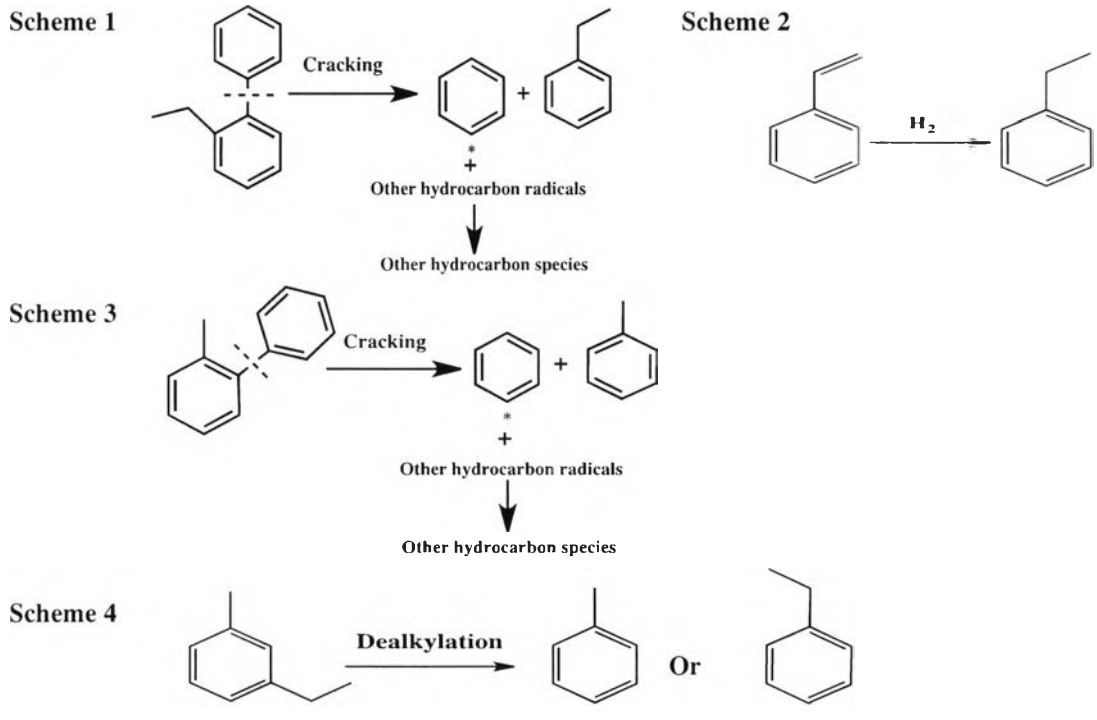

Figure 8.12 Possible reaction schemes for transformation of ethylbiphenyl, methylbiphenyl, styrene and 1-ethyl-3-methyl-benzene to valuable aromatics.

Moreover, the concentration of styrene has been found to significantly decrease, so the styrene might react with available H_2, forming ethylbenzene as displayed in **Scheme 2.** Moreover, toluene can be formed from cracking of methylbiphenyl as displayed in **Scheme 3.** Benzene can also be a product of cracking of methylbiphenyl, but it has not been found to increase, so it might convert to other hydrocarbon species via free radicals. In addition the concentration of 1-ethyl-3methyl-benzene significantly decreases, so the dealkylation of 1-ethyl-3methyl-benzene might take place, resulting in the high formation of toluene and ethylbenzene (see **Scheme 4**). **Schemes 1 and 3** likely take place on both MCM-41 shell and HY core since the pure MCM-41 and HY zeolite also reduce the formation of ethylbiphenyl (see Figure 8.11(b)). In addition, **Schemes 2 and 4** likely occur by

the synergy of MCM-41 shell and HY core since the pure MCM-41 and HY zeolite do not suppress the formation of styrene and ethylmethylbenzene.

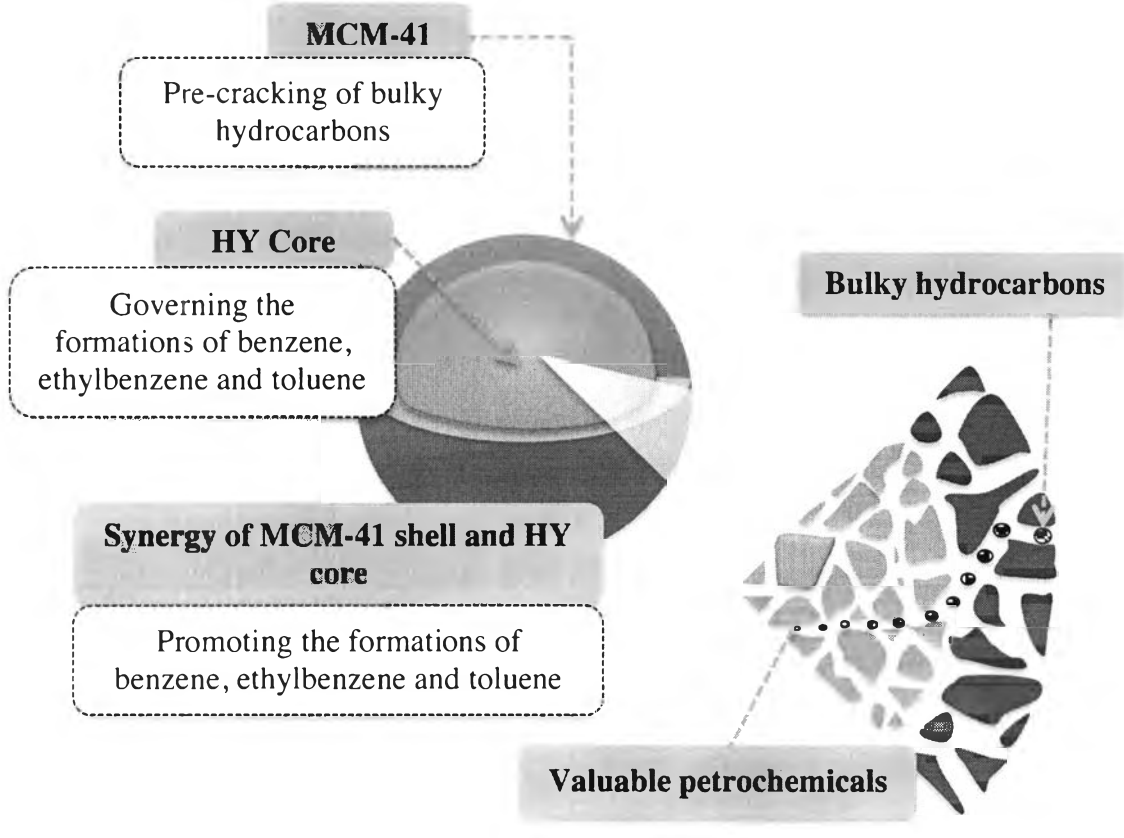

Figure 8.13 Role of core-shell composite of HY and MCM-41.

8.4.4 Sulfur Content in Oils

The sulfur content in oils clearly decreases with the presence of catalysts. The sulfur contents in oils obtained from HY zeolite and MCM-41 nearly are equal. These results indicate that the different pore sizes of these two catalysts do not have strong effect on the desulfurization of tire-derived oil. On the other hand, the connection of HY core with MCM-41 shell slightly provides a lower sulfur content in oil than those obtained from pure HY and MCM-41 since some sulfur-containing compounds might be cracked at weak acid sites located on MCM-41 shell, and the resulting products might diffuse to the HY zeolite core and then are desulfurized at strong acid sites located on the HY core. Therefore, the composite

catalyst provides a higher possibility of desulfurization of sulfur-containing compounds due to combination of different acidity. The composite catalyst favors to break C-S and C-N bond of sulfur-containing compounds in oil, leading to high sulfur distribution in the gas products (see Figure 8.14(b)).

Table 8.2 Sulfur contents in pyrolysis oil from using HY, MCM-41 and the HY/MCM-41 core-shell composite

Catalyst	Non-catalyst	HY	MCM-41	HY/MCM-41
Sulfur content in oil (wt%)	0.96	0.88	0.88	0.83
Sulfur reduction (%)	Base	8.3	8.3	13.5

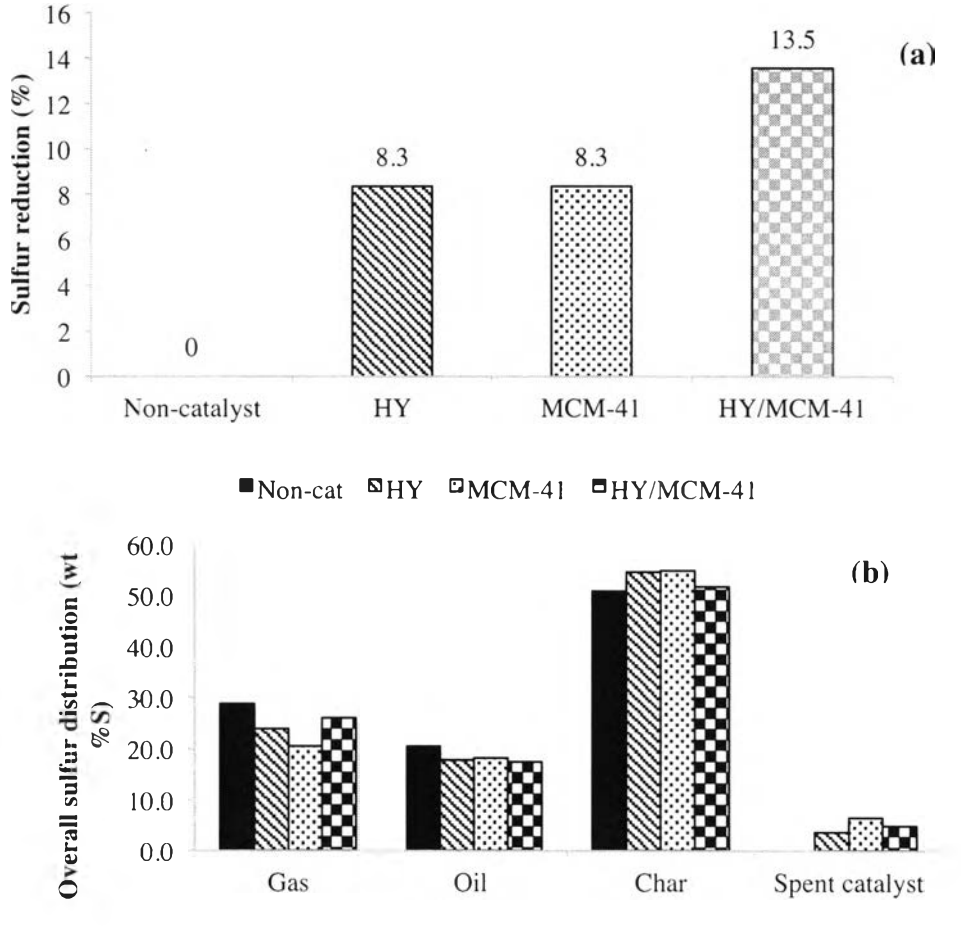

Figure 8.14 Sulfur reduction (a), overall sulfur distribution on pyrolysis products and spent catalysts (b), and Distribution of sulfur-containing compounds in maltenes from using HY, MCM-41 and their core-shell composite (c).

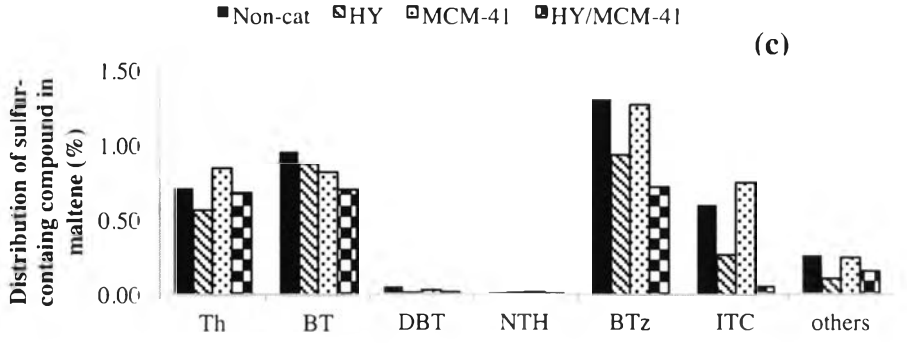

Figure 8.14 Sulfur reduction (a), overall sulfur distribution on pyrolysis products and spent catalysts (b), and Distribution of sulfur-containing compounds in maltenes from using HY, MCM-41 and their core-shell composite (c). (Con't.)

Sulfur-containing compounds in maltene are classified into six groups (Yuwapornpanit and jitkarnka, 2015); that are, thiophenes (Th), benzothiophenes (BT), dibenzothiophene (DBT), napthothiophenes (NT), benzothiazoles (BTz), isothiocyanates (ITC) as displayed in Figure 8.14(c). The pure HY catalyst, which possesses strong acid sites and micropore, can decrease the formation of thiophenes, benzothiophenes, benzothiazoles, and isothiocyanates since the pore size of HY allows thiophenes, benzothiophene, benzothiazoles and isothiocynates to diffuse inside the zeolite channel to be desulfurized. On the other hand, the presence of MCM-41, which possesses a large pore size and weak acid sites, slightly decreases the formation of benzothiophenes and benzothiozoles as compared to pure HY. Moreover, the formations of thiophenes and isothiocynates significantly increase as compared to thermal pyrolysis and HY zeolite. These results can be explained by two reasons; (i) the large pore size of MCM-41 catalyst might promote the cracking of heavy sulfur-containing compounds, such as DBT, NTH and etc, resulting in the high formation of slightly smaller sulfur-containing compounds, such as thiophenes and isothiocynates; and (ii) the acidity of MCM-41 is weaker than HY zeolite, so it cannot sufficiently break C-S bond and C-N bond of benzothiazoles and isothiocyanates, resulting in the higher formation of isothiocyanates and benzothiazoles.

Significant changes are observed in the formation of sulfur-containing compounds with using the core-shell composite of HY and MCM-41. The presence of composite catalyst provides a lower the formation of thiophenes, benzothiophene, benzothiazoles and isothiocyanates than the pure HY and MCM-41 catalysts. These results indicate that the combination of MCM-41 shell that possesses the weak acid sites and large pore size, and HBETA core with strong acid sites and micropore can overcome the limitation of zeolite and MCM-41 on desulfurization of sulfur-containing compounds. The limitation of zeolite is that zeolites possesses a small pore size that cannot allow the some sulfur-containing compounds such as DBT, NTH, BTZ and ITC to be effectively desulfurized in the zeolite channel. The limitation is that MCM-41 possesses only weak acid sites that cannot effectively desulfurized and denitrogenize BTz and ITC. Moreover, the formations of all sulfur-containing compounds are lower than MCM-41 catalyst since the core-shell composite provides a higher possibility for desulfurization of sulfur-containing compounds. The bulky sulfur-containing compounds might be desulfurized at the weak acid site of MCM-41 shell, and the slightly smaller sulfur compounds are further desulfurized at the strong acid sites of HY core, leading to the a higher desulfurization activity than MCM-41 and HY catalysts. (See Figure 8.15).

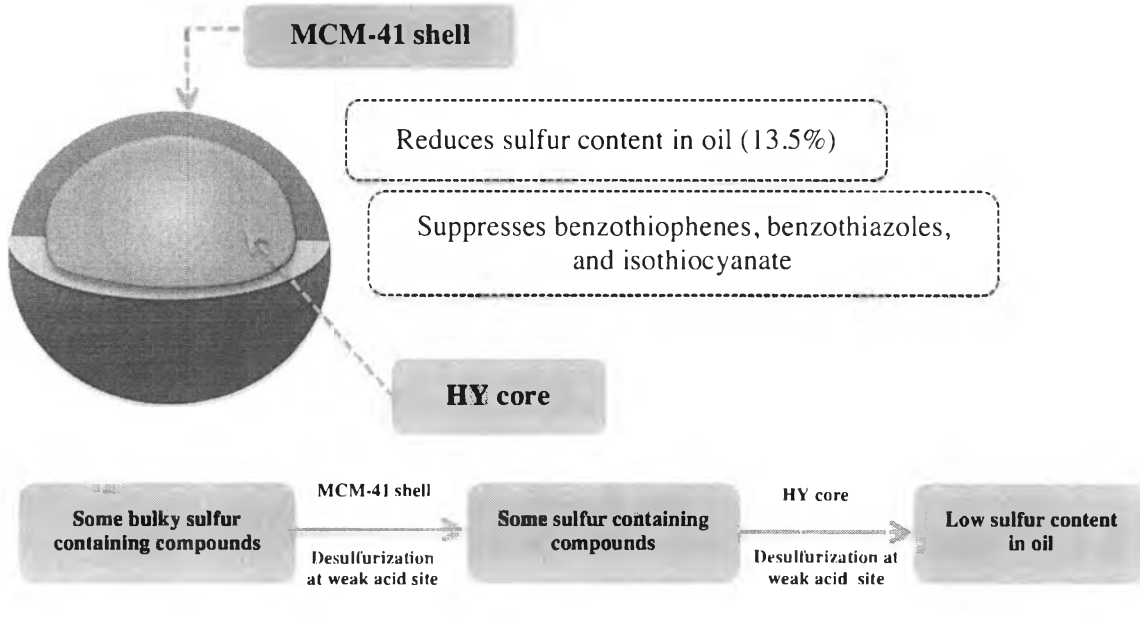

Figure 8.15 Role of core-shell composite on sulfur removal from tire-derived oil.

8.5 Conclusions

The core-shell composite comprising of HY zeolite core and mesoporous MCM-41 shell with a thin shell thickness (50-100 nm.) can be considered a promising catalyst for enhancement of quality of tire-derived oil in terms of reduction of polycyclic aromatics, enhancement of petrochemical production and sulfur reduction. The results indicate that the core-shell composite catalyst strongly promoted the production of gasoline, indicating that the cracking activity on the composite catalysts was higher than the pure HY and MCM-41 catalysts. Moreover, the formation of di-, poly- and polar-aromatics in oil significantly decreased as compared to pure HY zeolite since these aromatics cannot be sufficiently cracked in the micropore of HY zeolite. Furthermore, the good balance between acidity and pore size of composite catalysts provided a lower formation of poly-and polar-aromatics in oil than pure HBETA. In addition, the core-shell composite catalyst provided an excellent catalytic performance in the transformation of hydrocarbons to valuable aromatics. The core-shell composite of HY and MCM-41 strongly enhanced the formation of ethylbenzene and toluene since the composite catalyst favored the production of petrochemicals via transformation of polycyclic aromatics and mono-aromatics to valuable aromatics. Furthermore, the composite catalyst also provided a lower sulfur tire-derived oil than the oil produced from pure MCM-41 and HY catalysts. Therefore, it is reasonable to conclude that the growth of mesoporous MCM-41 layer around microporous HY zeolite particles, forming a bimodal pore distribution, exhibited the excellent potential in enhancement of quality of waste tire-derived oil with a high proportions of gasoline and petrochemicals.

8.6 Acknowledgements

The author would like to thank The Petroleum and Petrochemical College, Chulalongkorn University, Thailand, Center of Excellence on Petrochemical and Materials Technology, and Thailand Research Fund (TRF) for financial supports.

8.7 References

Bordoloi, A., Devassy, B.M., Niphadkar, P.S., Joshi, P.N., and Halligudi, S.B. (2006) Shape selective synthesis of long-chain linear alkyl benzene (LAB) with AlMCM-41/Beta zeolite composite catalyst. Journal of Molecular Catalysis A: Chemical, 253(1-2), 239-244

Boxiong, S., Chunfei, W., Binbin, G., Rui, W., and Cai, L. (2007) Pyrolysis of waste tyres with zeolite USY and ZSM-5 catalysts. Applied Catalysis B: Environmental, 73(1-2), 150-157.

Dũng, N.A., Klaewkla, R., Wongkasemjit, S., and Jitkarnka, S. (2009) Light olefins and light oil production from catalytic pyrolysis of waste tire. Journal of Analytical and Applied Pyrolysis, 86(2), 281-286.

Dũng, N.A., Tanglumlert, W., Wongkasemjit, S., and Jitkarnka, S. (2010) Roles of ruthenium on catalytic pyrolysis of waste tire and the changes of its activity upon the rate of calcination. Journal of Analytical and Applied Pyrolysis, 87(2), 256 262.

Jia, L., Sun, X., Ye, X., Zou, C., Gu, H., Huang, Y., Niu, G., and Zhao, D. (2013) Core shell composites of USY@Mesosilica: Synthesis and application in cracking heavy molecules with high liquid yield. Microporous and Mesoporous Materials, 176, 16-24.

Li, X., Zhou, F., Wang, A., Wang, L., and Hu, Y. (2009) Influence of Templates on the Overgrowth of MCM-41 over HY and the Hydrodesulfurization Performances of the Supported Ni-Mo Catalysts. Industrial& Engineering. Chemistry Research, 48, 2970-2877.

Manchantrarat, N. and Jitkarnka, S. (2012) Impact of HY as an additive in Pd/HBETA catalyst on waste tire pyrolysis products. Chemical Engineering Transactions, 29, 733-738.

Muenpol, S., Yuwapornpanit, R., and Jitkarnka, S. (2015) Valuable petrochemicals, petroleum fractions, and sulfur compounds in oils derived from waste tyre pyrolysis using five commercial zeolites as catalysts: Impact of zeolite properties. Cleaner Technology and Environmental Policy, DOI 10.1007/s10098-015-0935-8.

Ooi, Y.-S., Zakaria, R., Mohamed, A.R., and Bhatia, S. (2004) Synthesis of composite material MCM-41/Beta and its catalytic performance in waste used palm oil cracking. Applied Catalysis A: General, 274(1-2), 15-23.

Ren, J., Wang, A., Li, X., Chen, Y., Liu, H., and Hu, Y. (2008) Hydrodesulfurization of dibenzothiophene catalyzed by Ni-Mo sulfides supported on a mixture of MCM- 41 and HY zeolite. Applied Catalysis A: General, 344(1-2), 175-182.

Wehatoranawee, A. and Jitkarnka, S. (2010, October) Effect of silver supported HMOR-zeolite on waste tire pyrolysis products. Paper presented at The Second Innovative Energy & Environmental Chemical Engineering, Laguna Beach Resort, Phuket, Thailand.

Yuwapornpanit, R. and Jitkarnka, S. (2015) Cu-doped catalysts and their impacts on tire-derived oil and sulfur removal. Journal of Analytical and Applied Pyrolysis, 111, 200-208.

Zhou, F., Li, X., Wang, A., Wang, L., Yang, X., and Hu, Y. (2010). Hydrodesulfurization of dibenzothiophene catalyzed by Pd supported on overgrowth-type MCM-41/HY composite. Catalysis Today, 150(3-4), 218-223.